JOURNAL OF ENVIRONMENTAL SCIENCE AND HEALTH, PART A
2017, VOL. 52, NO. 8, 804–818
http://dx.doi.org/10.1080/10934529.2017.1305181

Taylor & Francis
Taylor & Francis Group

Nitrogen removal and its relationship with the nitrogen-cycle genes and microorganisms in the horizontal subsurface flow constructed wetlands with different design parameters

Jun Chen, Guang-Guo Ying, You-Sheng Liu, Xiao-Dong Wei, Shuang-Shuang Liu, Liang-Ying He, Yong-Qiang Yang, and Fan-Rong Chen

State Key Laboratory of Organic Geochemistry, CAS Research Centre for Pearl River Delta Environmental Pollution and Control, Guangzhou Institute of Geochemistry, Chinese Academy of Sciences, Guangzhou, China

ABSTRACT

This study aims to investigate nitrogen removal and its relationship with the nitrogen-cycle genes and microorganisms in the horizontal subsurface flow constructed wetlands (CWs) with different design parameters. Twelve mesocosm-scale CWs with four substrates and three hydraulic loading rates were set up in the outdoor. The result showed the CWs with zeolite as substrate and HLR of 20 cm/d were selected as the best choice for the TN and NH_3-N removal. It was found that the single-stage mesocosm-scale CWs were incapable to achieve high removals of TN and NH_3-N due to inefficient nitrification process in the systems. This was demonstrated by the lower abundance of the nitrification genes (AOA and AOB) than the denitrification genes (*nir*K and *nir*S), and the less diverse nitrification microorganisms than the denitrification microorganisms in the CWs. The results also show that microorganism community structure including nitrogen-cycle microorganisms in the constructed wetland systems was affected by the design parameters especially the substrate type. These findings show that nitrification is a limiting factor for the nitrogen removal by CWs.

ARTICLE HISTORY
Received 9 January 2017
Accepted 16 February 2017

KEYWORDS
Constructed wetland; denitrification; nitrification; nitrogen-cycle genes; nitrogen-cycle microorganisms; nitrogenous substances

Introduction

Constructed wetlands (CWs) are artificial wetlands that are designed and constructed to manipulate the natural processes to treat wastewater by utilizing wetland plants, soil, and associated microorganisms, and can be classified into surface flow and subsurface flow wetlands (vertical or horizontal) according to their hydrology and flow path. Previous studies demonstrated that CWs are capable of removing various environmental pollutants including nitrogen, phosphorous, heavy metals,[1–3] and antibiotics and ARGs [4,5] through physical process (filtration, physical adsorption, and volatilization), chemical process (precipitation, ion-exchange, and oxidation-reduction reaction) and biological process (plant uptake and microbial degradation).[6–9] Their performance depends on the design parameters such as substrates, hydraulic loading rates, plant species, flow types, hydraulic retention time, applied pollutants loadings and so on.[10–14]

CWs have shown variable removal rates for nitrogenous substances, and often produce unsatisfactory treatment results for nitrogenous substances.[13,15–17] The nitrogen removal rate by a typical CW was reported only 35%, and still under 50% even with an optimized design in Europe;[18] while an average of 44% nitrogen removal rate in CWs was documented in North America.[19] Hence, it is very important to understand the removal mechanism of nitrogen pollutants to further enhance their removal efficiency in constructed wetlands.

Nitrogen removal in CWs involves physical process, chemical process and microbial process including NH_3-N volatilization, nitrification, denitrification, nitrogen fixation, plant and microbial uptake, mineralization (ammonification), nitrate reduction to ammonium (nitrate-ammonification), anaerobic ammonia oxidation (anammox), fragmentation, sorption, desorption, burial, and leaching.[15] However, microbial processes especially nitrification and denitrification were found to be the driving force in these systems to decrease nitrogen.[20–22] Nitrification is usually defined as the oxidation of ammonium (NH_3-N) to nitrate (NO_3^-) with nitrite (NO_2^-) as an intermediate in the reaction sequence by nitrifying microorganism, while denitrification is most commonly defined as the process in which nitrate (NO_3^-) is converted into dinitrogen (N_2) via intermediates nitrite (NO_2^-), nitric oxide (NO^-) and nitrous oxide (N_2O^-) by denitrifying microorganism.[23]

With the development of molecular biological technique, nitrogen-cycle genes and microorganisms have received increasing attention in recent years. Previous studies demonstrated that both ammonia-oxidizing bacteria (AOB) and archaea (AOA) contributed to nitrification by quantifying the abundance of the genes encoding a subunit of the key enzyme ammonia monooxygenase (*amoA*) using polymerase chain reaction (PCR) in the ocean,[24–26] wastewater treatment

CONTACT Guang-Guo Ying guang-guo.ying@gig.ac.cn; guangguo.ying@gmail.com State Key Laboratory of Organic Geochemistry, CAS Research Centre for Pearl River Delta Environmental Pollution and Control, Guangzhou Institute of Geochemistry, Chinese Academy of Sciences, 511 Kehua Street, Tianhe District, Guangzhou 510640, China.

Color versions of one or more of the figures in the article can be found online at www.tandfonline.com/lesa.

plants,[27,28] soils,[29,30] as well as natural wetlands,[31,32] but rarely in constructed wetlands.[33] Microbial denitrification consists of four consecutive reaction steps, that is, NO_3^- (*narG* or *napA*) → NO_2^- (*nirS* or *nirK*) → NO^- (*norB*) → N_2O^- (*nosZ*) → N_2.[24,34] Chon et al.[33] reported nitrite-reducing functional genes (i.e., *nirS*) were dominant over the other two genes (*narG* and *nosZ*) in the effluent-fed wetland. However, the previous studies focus on explaining the nitrogen removal mechanism by wetlands from the gene level, the abundance and diversity of nitrogen-cycle functional microorganisms in CWs is still unknown. Thus, it is essential for us to better understand the abundance of nitrogen-cycle genes and diversity of nitrogen-cycle microorganisms in the black box of CWs in order to improve the capacity of CWs for nitrogen removal.

The objectives of this study were: (1) to investigate the removal of nitrogenous substances (TN: total nitrogen and NH_3-N: ammonium nitrogen) in domestic wastewater by 12 mesocosm-scale CWs with different design parameters (subsurface flow, three hydraulic loading rates (HLR = 10, 20 and 30 cm/d) and four substrates (oyster shell, zeolite, medical stone and ceramic)); (2) to explore the abundance of four nitrogen-cycle genes, that is ammonia monooxygenase (*amoA*) of bacteria (AOB) and archaea (AOA) and nitrite reductase (*nirK* and *nirS*) in the mesocosm-scale CWs by qPCR analysis; and (3) to reveal the diversity of nitrogen-cycle functional microorganisms in the black box of mesocosm-scale CWs by high-throughput sequencing. The results from this study can help understand nitrogen removal mechanism in molecular level, and improve the nitrogen removal capacity by CWs.

Materials and methods

Setup of the mesocosm-scale constructed wetlands

Twelve mesocosm-scale CWs were set up in the outdoor within the campus of Guangzhou Institute of Geochemistry (GIG) in Guangzhou City, south China. Guangzhou is located at 113.3° east longitude and 23.1° north latitude, which is in the subtropical monsoon climate zone. Annual temperature is about 21.4–21.9°C, and annual precipitation is about 1624–1900 mm. All the mesocosm-scale CWs were built each with a stainless steel container (60 cm wide, 80 cm long and 80 cm high), planted with *Cyperus alternifolius* L. (6 plants in two rows in each system), and operated with horizontal subsurface flow (Fig. 1). The mesocosm-scale CWs differed in substrate and hydraulic loading rate. The four substrates used in the CWs included oyster shell (irregular shape, void fraction approximately 34.2%), zeolite (grain size 2–3 cm, void fraction 44.7%), medical stone (grain size 2–3 cm, void fraction 46.5%), and ceramic (grain size 2–3 cm, void fraction 42.6%), while the HLRs applied were controlled by flowmeters at 10, 20 and 30 cm/day. Furthermore, each mesocosm-scale CW had a layer of 65 cm substrate and a layer of 60 cm water within the substrate. In each mesocosm-scale CW, approximately 7.5×10^4 g oyster shell, or 5.5×10^5 g zeolite, or 4.0×10^5 g medical stone, or 3.0×10^5 g ceramic was used.

The mesocosm-scale CWs were built to treat raw domestic sewage from the residential area in GIG campus with about 330 people. All the raw domestic sewage was collected by a sewer line and then fed through a stainless steel regulating pool of 4.3 m^3 to the wetlands. The mesocosm-scale CWs have been working well since September 2013 as shown by the weekly water quality parameters monitoring. The experiment was performed in November 2014.

Sample collection

In order to avoid the dilution of raw domestic sewage by rainwater, more than 15 days without rain before the sample collection were ensured. In the sampling campaign, we collected 13 wastewater samples and 12 solid samples. The

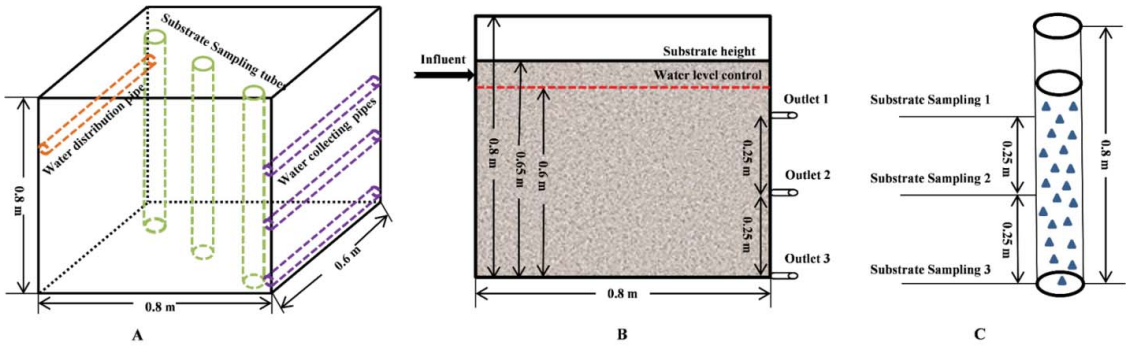

	Substrates			
HLR (cm/d)	Oyster shell	Zeolite	Medical stone	Ceramic
10	CW1	CW4	CW7	CW10
20	CW2	CW5	CW8	CW11
30	CW3	CW6	CW9	CW12

Figure 1. The design of mesocosm-scale constructed wetlands showing sampling locations. The table under the design scheme shows all 12 constructed wetlands. (a) Constructed wetland stereogram, (b) water sample collection, and (c) substrate sample collection. HLR: hydraulic loading rate.

effluent samples and substrate samples were named as follows: Wx (effluent) and Sx (substrate) from CWx (wetland x: 1–12), with their influent as W0 (the same for all 12 CWs). Thirteen wastewater samples were collected as the 72-h composite samples (sampling once every 8 h) during a 3-d period. The water samples were collected from the influent and effluent of the water outlet 3 (Fig. 1b) for the analysis of nitrogenous substances, and composite samples of three water outlets' effluent (Fig. 1b) for the analysis of nitrogen-cycle genes (Fig. 1b). Twelve solid samples were collected only one time from the three substrate sampling points (Fig. 1c) after wastewater sampling and then mixed into the composite samples according to their depths (there were three sampling tubes in each CW, and each had three sampling depths) (Fig. 1a and c). One gram of sodium azide was added to each substrate sample to suppress microbial activity. All the samples were then kept refrigerated and transported to the laboratory as soon as possible, where they were stored at 4°C before analysis (within 48 h). The substrate samples were freeze-dried, homogenized, and passed through a 60-mesh standard sieve and then kept at −20°C in the dark until extraction.

Chemical analysis

General wastewater quality parameters (pH, DO, temperature, conductivity and redox potential) were monitored onsite by the YSI meter (YSI-Pro2030; YSI Incorporated, Yellow Springs, OH, USA), while nitrogenous substances were determined according to Chinese standard methods. The standard methods were listed as follows: TN: total nitrogen[35] (HJ 636-2012: Alkaline potassium persulfate digestion-UV spectrophotometric method); NH_3-N: ammonia nitrogen[36] (HJ 536-2009: Nessler's reagent spectrophotometry); NO_3^-: nitrate nitrogen[37] (GB/T 7480-1987: Spectrophotometric method with phenol disulfonic acid); NO_2^-: nitrite nitrogen[38] (GB/T 7493-1987: Spectrophotometric method). All nitrogenous substances were determined by a UV–vis spectrophotometer (Shimadzu Instrument Co. Ltd., UV-2450, Japan).

Extraction and quantification of nitrogen-cycle genes

For water samples, 0.5 L each was filtered through a sterile membrane filter (0.45-μm pore diameter) with a vacuum filtration apparatus, and the membrane filters were aseptically kept for total DNA extraction. For substrate samples, 10 g each was extracted by 50 mL of 0.85% sterile stroke-physiological saline three times, then the saline was filtered through a sterile membrane filter (0.45-μm pore diameter) with a vacuum filtration apparatus; and the membrane filters were aseptically kept for total DNA extraction. Total DNA from the water and substrate samples was extracted by the PowerSoil DNA Isolation Kit (Mo Bio Laboratories, Carlsbad, CA, USA) by following the manufacturer protocol, and further purified using the DNA Spin Kit (Tiangen Biotech, China) to minimize PCR inhibition.

Real-time quantitative polymerase chain reaction (qPCR) was used to quantify the six target genes including the 16S ribosomal RNA (16S rRNA) of bacteria and archaea, and four nitrogen-cycle genes, that is ammonia monooxygenase (*amoA*) of bacteria (AOB) and archaea (AOA) and nitrite reductase (*nirK* and *nirS*). The specific primers, annealing temperatures and expected amplicon sizes for the target genes are listed in Table A1. The qPCR assays were run on ViiA^{TM} 7 Real-Time PCR System (ABI, Foster City, CA, USA) using SYBR Green Real-Time QPCR Kit (TAKARA, Japan). The detailed DNA extraction, purification and nitrogen-cycle genes quantification (SI Text S1) methods can be referred to our previous study.[5,39,40]

High-throughput sequencing for microbial community analysis and nitrogen-cycle microorganisms

The substrate samples of S2, S4, S5, S6, S8, and S11 from all the CWs with HLR 20 cm/d and those CWs with zeolite as the substrate were chosen for the microbial community analysis. And the primer set 515F (50-GTGCCAG-CAGCCGCGGTAA-3′) and 806R (50-GGACTACCAGGG-TATCTAAT-38) with the barcode that amplifies the V4 region of the 16S rDNA were used. All PCR reactions were carried out with Phusion® High-Fidelity PCR Master Mix (New England Biolabs, Ipswich, MA, USA). The PCR reactions in a 50 μL mixture contained 20 μL Premix Ex Taq (Takara Biotechnology), 0.4 μL of each primer (10 μM), 4 μL of fivefold diluted template DNA (1–10 ng), and 25.2 μL sterilized water. Thermal-cycling conditions were as follows: an initial denaturation of 3 min at 94°C, six touchdown cycles of 45 s at 94°C, 60 s from 65°C to 58°C, 70 s at 72°C, followed by 22 cycles of 45 s at 94°C, 60 s at 58°C, 60 s at 72°C with a final elongation of 72°C for 10 min. The same volume of 1X loading buffer (contained SYB green) was mixed with PCR products; electrophoresis was performed on 2% agarose gel for detection. Samples with bright main strips between 400 and 450 bp were chosen for further experiments. PCR products were mixed in equidensity ratios. Then, the mixture of PCR products was purified with Qiagen Gel Extraction Kit (Qiagen, Germany). Sequencing libraries were generated using TruSeq® DNA PCR-Free Sample Preparation Kit (Illumina, USA) following manufacturer's recommendations, and index codes were added. The library quality was assessed on the Qubit@ 2.0 Fluorometer (Thermo Scientific) and Agilent Bioanalyzer 2100 system. At last, the library was sequenced on an Illumina HiSeq 2500 platform, and 250-bp paired-end reads were generated by Novogene (Beijing, China).

The total DNA in each substrate sample was also sequenced for nitrogen-cycle microorganisms with specific nitrogen-cycle functional genes with the primers (*amoA* for nitrification: *amoA*-1F: GGGGTTTCTACTGGTGGT, *amoA*-2R: CCCCTCKGSAAAGCCTTCTTC;[41] *nosZ* for denitrification: *nosZ*-F: CGYTGTTCMTCGACAGCCAG, *nosZ*1622R: CGSACCTTSTTGCCSTYGCG [42]). The PCR reactions in a 50 μL mixture contained 4 μL dNTP (2.5 mM), 5 μL 10◊*Pyrobest* buffer, 0.3 μL *Pyrobest* DNA Polymerase (2.5 U/μL, Takara code: DR005A), 2 μL of each primer (10 μM), x μL template DNA (30 ng) and (36.7-x) μL sterilized water. Thermal-cycling conditions were as follows: an initial denaturation of 5 min at 95°C,

followed by 25 cycles of 30 s at 95°C, 30 s at 56°C, 40 s at 72°C with a final elongation of 72°C for 10 min, then ended at 4°C. The PCR products were purified using magnetic beads, and the concentrations of the PCR products were fluorometrically quantified by the Qubit dsDNA HS Assay Kit (Qubit2.0, Life Technologies, CA, USA) before being sequenced on the Miseq platform (Illumina, San Diego, CA, USA) by Beijing Honor Tech Co., Ltd., China. The tags were obtained by joining the reads according to the connection of overlap by COPE (Connecting Overlapped Pair-End, V1.2.3.3), then wiped off the barcode sequences and primer sequences to get the raw tags. After that, the tags less than 200 bp and chimera were expurgated to obtain the clean tags. Clean tags were quality trimmed and clustered into operational taxonomic units (OTUs) at a 97% identity threshold using uclust in QIIME V1.7.0 (http://qiime.org/index.html). The tags were compared with the reference database (Gold database, http://drive5.com/uchime/uchime_download.html) using UCHIME algorithm (UCHIME Algorithm, http://www.drive5.com/usearch/manual/uchime_algo.html) to detect chimera sequences, and then the chimera sequences were removed. Then the Effective Tags were finally obtained. Non-singletons OUTs were collected after removal of the meaningless singletons OUTs for the downstream analyses. For each representative sequence, the GreenGene Database (http://greengenes.lbl.gov/cgi-bin/nph-index.cgi) was used based on RDP classifier (Version 2.2, http://sourceforge.net/projects/rdp-classifier/) algorithm to annotate taxonomic information. In order to study phylogenetic relationship of different OTUs, and the difference of the dominant species in different samples (groups), multiple sequence alignment was conducted using the MUSCLE software (Version 3.8.31, http://www.drive5.com/muscle/). Alpha diversity analysis, Beta diversity analysis, principal component analysis (PCA), cluster analysis, and microorganism community distribution analysis were conducted for the purpose of uncovering the abundance and diversity of nitrogen-cycle microorganisms in the black box of mesocosm-scale CWs.

Mass loading analysis and gene amounts analysis

Mass loading analysis was applied to investigate the removal efficiency of the mesocosm-scale CWs under different conditions. This analysis determines the mass flow of a pollutant entering and leaving each mesocosm-scale CW in water phase by multiplying concentrations of each pollutant in aqueous phase by average daily flow.

$$M_i = C_{i,\ water} \times Q \quad (1)$$

where M_i is the mass loading of the pollutant i in the water phase, $C_{i,\ water}$ represents the concentration of pollutant i in water, and Q is the average daily water flow in the mesocosm-scale CWs.

$$M_{removal} = M_{influent} - M_{effluent} \quad (2)$$

where $M_{influent}$ and $M_{effluent}$ are the mass loadings (aqueous phase) of a pollutant in the influent and each mesocosm-scale CW effluent, respectively; and $M_{removal}$ is the mass removal of the pollutant after mesocosm-scale CW treatment.Gene amounts of the mesocosm-scale constructed wetlands are calculated as:

$$B_{i,j} = C_{i,j,\ substrate} \times M_i + C_{i,j,\ water} \times V_i \quad (3)$$

where $B_{i,j}$ is the gene amounts of CW with substrate i and HLR j, $C_{i,j,\ substrate}$ represents the concentration of target genes in substrate (CW with substrate i and HLR j), $C_{i,j,\ water}$ represents the concentration of target genes in water (CW with substrate i and HLR j), and M_i is the total mass of substrate i and V_i is the volume of water in the mesocosm-scale CWs with substrate i.

Statistical analysis

Basic data analysis was performed with Microsoft Excel 2010 to obtain averages and standard deviations of concentrations of target nitrogen-cycle genes. Spearman's rank test was used to investigate the statistical correlation between the removal of nitrogenous substances and abundance of nitrogen-cycle genes using SPSS version 20.0 (IBM, NY). In order to reveal Alpha diversity in each substrate samples, Shannon index, Chao1 index, Phylogenetic diversity (PD, whole tree) and observed number of species were characterized by QIIME V1.7.0 and displayed with R software (Version 2.15.3). The principal component analysis (PCA), cluster analysis, unweighted pair-group method with arithmetic mean (UPGMA) analysis, non-metric multi-dimensional scaling (NMDS) analysis, and microorganism community distribution histogram were performed with R software (Version 2.15.3).

Results

Operational performance of the mesocosm-scale CWs

Nitrogenous substances in water and substrate samples of the mesocosm-scale CWs are summarized in Table 1. Nitrogenous substances TN, NH_3-N, NO_3^- and NO_2^- were detected in the substrate samples, with the concentrations ranging from 126 to 1060 mg/kg, from 7.48 to 328 mg/kg, from 3.74 to 82.2 mg/kg and from 0.01 to 1.41 mg/kg, respectively. The 12 mesocosm-scale CWs showed variable removals of TN and NH_3-N ranging between 16.1% and 45.9% and between 9.2% and 34.8%, respectively. It can be seen that that the aqueous removal rates for TN and NH_3-N decreased with increasing HLR.

The mass loadings of pollutants in the influent and effluent were calculated to indicate the treatment efficiency of the CWs. The mass loadings and mass removals of TN and NH_3-N by the mesocosm-scale CWs are summarized in Table 2. The calculated total mass loadings of TN and NH_3-N in the influent were 2.64 and 1.43 g/d, 5.27 and 2.85 g/d, 7.80 and 4.22 g/d for HLR 10, 20 and 30 cm/day, respectively, and after treatment the total mass loadings in the effluents were reduced to 1.47–2.02 and 0.93–1.11 g/d, 3.00–3.95 and 2.19–2.53 g/d, 5.85–6.58 and 3.42–3.83 g/d, respectively (Table 2). Daily mass removals of TN and NH_3-N in raw wastewater increased with increasing HLR by the mesocosm-scale CWs under the same substrate.

Table 1. Concentrations and removal rates of nitrogenous substances in the mesocosm-scale constructed wetlands.

			Water samples (mg/L)				Substrate samples (mg/kg)			
			TN[a]	NH_3-N[b]	NO_3^-[c]	NO_2^-[d]				
Influent			54.9	29.7	0.20	0.04	TN	NH_3-N	NO_3^-	NO_2^-
Effluent	Oyster Shell	HLR = 10[e]	30.6 (44.3)[f]	20.1 (32.5)	1.12 (−463)	0.01 (73.1)	1010	37.4	3.74	0.04
		HLR = 20	39.5 (28.0)	22.9 (23.1)	0.60 (−200)	0.12 (−185)	921	18.7	22.4	0.01
		HLR = 30	45.2 (17.7)	25.3 (14.8)	0.30 (−50.0)	0.01 (−87.3)	1060	18.7	7.48	0.02
	Zeolite	HLR = 10	32.6 (40.6)	19.4 (34.8)	0.15 (25.0)	0.09 (−118)	545	328	26.2	0.05
		HLR = 20	31.3 (43.0)	23.2 (22.0)	0.30 (−50.0)	0.05 (−25.9)	553	272	82.2	0.04
		HLR = 30	41.2 (24.9)	24.1 (19.0)	0.37 (−87.5)	0.06 (−40.1)	675	291	33.6	0.05
	Medical stone	HLR = 10	42.1 (24.9)	23.2 (19.0)	0.45 (−87.5)	0.11 (−40.1)	303	272	37.4	0.22
		HLR = 20	41.2 (23.3)	24.5 (22.0)	0.22 (−125)	0.04 (−160)	281	56.1	11.2	0.02
		HLR = 30	46.4 (25.0)	25.9 (17.5)	0.37 (−12.5)	0.01 (9.45)	155	37.4	11.2	0.08
	Ceramic	HLR = 10	29.7 (45.8)	22.8 (23.5)	1.20 (−500)	0.20 (−376)	178	29.9	26.2	1.41
		HLR = 20	37.9 (30.9)	26.3 (11.5)	0.07 (62.5)	0.08 (−82.5)	145	7.48	3.74	0.92
		HLR = 30	46.1 (16.1)	27.0 (9.21)	0.37 (−87.5)	0.07 (−57.8)	126	15.0	15.0	0.02

[a]Total nitrogen; [b]ammonia nitrogen; [c]nitrate nitrogen; [d]nitrite nitrogen; [e]hydraulic loading rate (cm/d); [f]concentrations (removal rates).

General wastewater quality parameters of the mesocosm-scale constructed wetlands are summarized in Table A2. As can be seen, the DO of the water phase in the CWs ranged from 0.22 to 0.72 mg/L, indicating low oxygen state (possibly reaching anaerobic or facultative anaerobic conditions) in the mesocosm-scale CWs.

Abundance of nitrogen-cycle genes

All the target genes including the 16S ribosomal RNA (16S rRNA) of bacteria and archaea, and four nitrogen-cycle genes, that is ammonia monooxygenase (*amoA*) of bacteria (AOB) and archaea (AOA) and nitrite reductase (*nirK* and *nirS*) were detected in both water and substrate samples from the mesocosm-scale systems (Fig. 2; Tables A3 and A4). The two most abundant genes in the water samples were 16S rRNA (bacteria) and *nirS*, with concentrations ranging from 1.81×10^9 to 8.73×10^9 copies/mL and from 1.60×10^8 to 1.86×10^9 copies/mL, respectively, following by 16S rRNA (archaea) and *nirK* ranging from 7.86×10^6 to 8.87×10^7 copies/mL and from 1.54×10^5 to 1.08×10^6 copies/mL, respectively, while AOA and AOB displayed the lowest abundance ranging from 1.85×10^5 to 3.34×10^5 copies/mL and from 1.19×10^5 to 8.48×10^5 copies/mL, respectively (Table A3). Meanwhile, the most abundant genes in the substrate samples were 16S rRNA (bacteria), 16S rRNA (archaea), and *nirS*, with concentrations ranging from 3.13×10^6 to 7.16×10^7 copies/g, from 5.77×10^6 to 1.15×10^8 copies/g, and from 1.18×10^7 to 9.74×10^7 copies/g, respectively, following by AOB, AOA and *nirK* ranging from 2.99×10^5 to 9.21×10^6 copies/g, from 1.99×10^5 to 3.29×10^6 copies/g, and from 6.36×10^5 to 9.52×10^6 copies/g, respectively (Table A4).

Considering the water volume, substrate weight and target gene abundance, the amount of nitrogen-cycle genes in each CW unit was calculated and is given in Figure 3 and Table A5. It is clear that bacteria were more abundant than archaea based on 16S rRNA analysis, and AOB showed higher levels than AOA in most CWs. In all the 12 CWs, *nirS* showed much higher levels than *nirK*.

Diversity of microbial community and nitrogen-cycle microorganisms

The substrate samples from all the CWs with HLR 20 cm/d and those CWs with zeolite as the substrate were chosen for the 16S rRNA gene sequencing to understand the effect

Table 2. Mass loadings and removal of the mass loadings of TN and NH_3-N in the mesocosm-scale constructed wetlands.

		TN[b] (g/d)		NH_3-N[c] (g/d)	
HLR[a]		Mass loadings	Removal	Mass loadings	Removal
10 cm/d	Influent	2.64	—	1.43	—
	Oyster shell	1.47	1.17	0.96	0.46
	Zeolite	1.57	1.07	0.93	0.50
	Medical stone	2.02	0.61	1.11	0.31
	Ceramic	1.43	1.21	1.09	0.34
20 cm/d	Influent	5.27	—	2.85	—
	Oyster shell	3.79	1.48	2.19	0.66
	Zeolite	3.00	2.27	2.23	0.63
	Medical stone	3.95	1.32	2.36	0.50
	Ceramic	3.64	1.63	2.53	0.33
30 cm/d	Influent	7.80	—	4.22	—
	Oyster shell	6.42	1.38	3.60	0.63
	Zeolite	5.85	1.94	3.42	0.80
	Medical stone	6.58	1.21	3.68	0.55
	Ceramic	6.54	1.26	3.83	0.39

[a]Hydraulic loading rate (cm/d); [b]total nitrogen; [c]ammonia nitrogen.

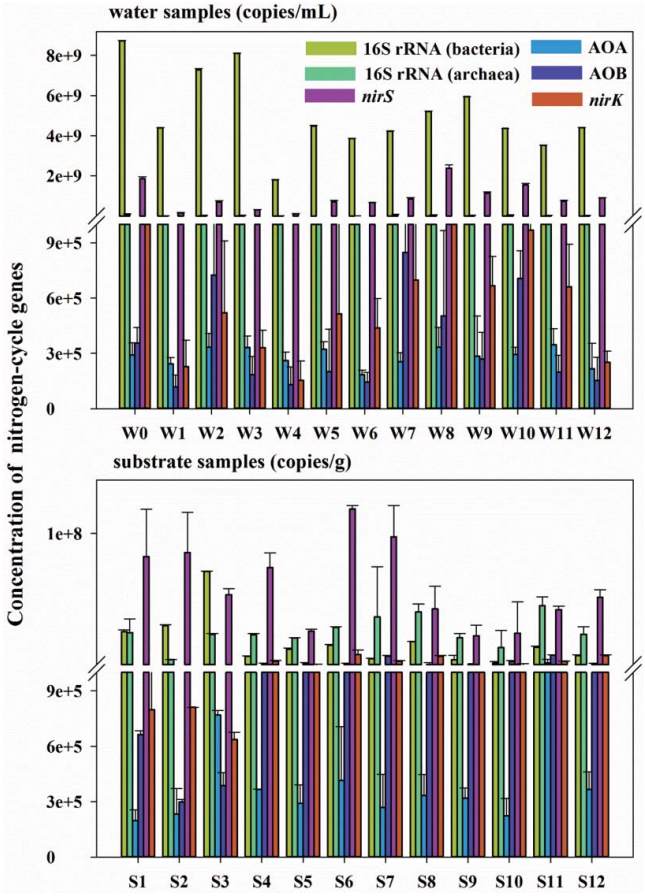

Figure 2. Absolute concentrations of nitrogen-cycle genes in the influent and effluents (copies/mL) and in the substrates (copies/g) of the mesocosm-scale constructed wetlands. Wx and Sx represent effluent and substrate samples from the constructed wetland CWx: Influent (W0), CW1 (W1 and S1), CW2 (W2 and S2), CW3 (W3 and S3), CW4 (W4 and S4), CW5 (W5 and S5), CW6 (W6 and S6), CW7 (W7 and S7), CW8 (W8 and S8), CW9 (W9 and S9), CW10 (W10 and S10), CW11 (W11 and S11), CW12 (W12 and S12).

of substrate types and HLRs on the diversity and structure of the bacterial community in the mesocosm-scale CWs. The sequencing results showed that *Proteobacteria, Firmicutes, Bacteroidetes, Actinobacteria* and *Verrucomicrobia* were the dominant bacteria in the CWs, followed by

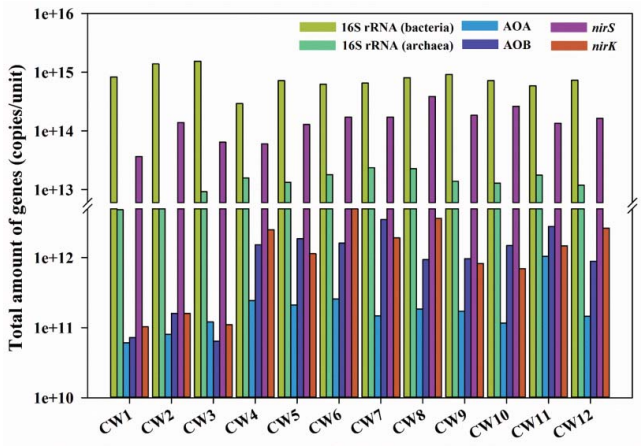

Figure 3. Gene amounts (copies/unit) of nitrogen-cycle genes in each mesocosm-scale constructed wetlands.

Chloroflexi, Planctomycetes, Acidobacteria, OP3 and *Spirochaetes* (Fig. A1). Meanwhile, the clustering analysis by UPGMA (Unweighted Pair-group Method with Arithmetic Mean) indicated that the microorganism community structure in the constructed wetland systems was affected by the design parameters such as substrate types and HLRs (Fig. A1). This was further proved by the NMDS (Non-Metric Multi-Dimensional Scaling) analysis based on the OTUs abundances of microorganism from the mesocosm-scale constructed wetlands (Fig. A2).

The DNA in the substrate from each CW was sequenced for the composition and diversity of nitrogen-cycle microorganisms. The raw tags, clean tags and OTUs of the substrate samples both *amoA* for nitrification and *nosZ* for denitrification are summarized in Table A6. The OTUs of *amoA* for nitrification ranged from 665 to 5926, while the OTUs of *nosZ* for denitrification ranged from 2340 to 5775. The nitrification and denitrification sequencing results showed that the ceramic substrate showed the highest OTUs, followed by zeolite and medical stone, and oyster shell had the lowest OTUs. Different OTUs among different substrate samples suggest that the HLRs and substrate types could affect the richness of nitrogen-cycle microorganisms in the mesocosm-scale CWs. This has further been confirmed by principal component analysis (PCA, Fig. 4) and the cluster analysis (Fig. A3) based on the OTUs abundances. The nitrification and denitrification microorganisms were grouped according to substrate materials, indicating different nitrogen-cycle microorganism community structure in the CWs with four different substrates (oyster shell, zeolite, medical stone and ceramic). However, overlapping of the zeolite substrate and the medical stone substrate (Fig. 4) implies their similarity to some extent in nitrogen-cycle microorganism community composition.

The composition and relative abundance of nitrogen-cycle microbial communities in genus level of the 12 substrate samples are shown in Figure 5. As shown in Figure 5, for nitrification, *Nitrosomonas* and *Nitrosospira* were the dominant genus in the mesocosm-scale CWs, but *Treponema* was the particular genus in the oyster shell systems. In contrast, more diverse denitrification microorganisms were observed in the CWs. In the oyster shell systems, *Azospirillum, Acidovorax, Massilia, Thauera* and *Pseudogulbenkiania* were the dominant genus, while *Azospirillum, Acidovorax, Bradyrhizobium* and *Pseudogulbenkiania* were the dominant genus in the other three substrate types systems (Fig. 5). Interestingly, *Pseudomonas, Rhodobacter, Paracoccus, Alcaligenes* and *Cupriavidus* were found to be the particular genus in the oyster shell systems, while *Mesorhizobium* was found in the other three substrate types systems but none in the oyster shell systems. In addition, *Alcaligenes* was found to be the particular genus in the ceramic systems.

Alpha diversity analysis including Chao index,[43] observed species,[44] phylogenetic diversity (PD, whole tree) [45,46] and Shannon index [47] were calculated by Alpha diversity analysis for the species diversity of substrate samples from the mesocosm-scale CWs, and the results are given in Table A7. For nitrification, the highest diversity indexes were found in the ceramic substrate, followed by zeolite, medical stone and oyster shell substrates. However, for denitrification, zeolite samples

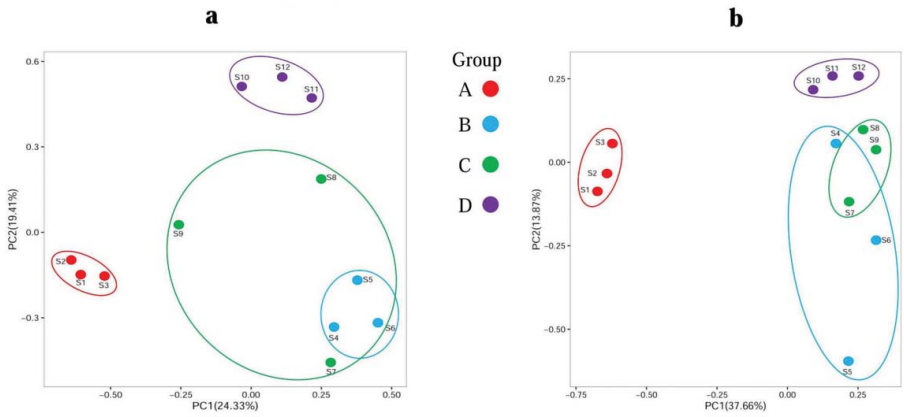

Figure 4. Principal component analysis (PCA) based on the OTUs abundances of (a) nitrification and (b) denitrification from the mesocosm-scale constructed wetlands. A–D represent the mesocosm-scale CWs with the substrate of oyster shell, zeolite, medical stone and ceramic, respectively.

had the highest diversity indexes, followed by medical stone, ceramic and oyster shell substrates.

Discussion

The results from the present study showed variable removals for the nitrogenous substances (TN, NH_3-N, NO_3^- and NO_2^-) by the mesocosm-scale CWs. The highest aqueous removal rates and mass removals for TN and NH_3-N were observed for the CWs with zeolite as substrate under the same HLR, and the aqueous removal rates for these two target pollutants decreased with increasing HLR (Tables 1 and 2). After considering their aqueous removal rates in combination with their mass removals, the CW with zeolite as the substrate and HLR of 20 cm/d was selected as the best choice for TN and NH_3-N removal. However, the single-stage mesocosm-scale CWs without optimization were incapable to achieve very high removals of TN and NH_3-N due to their inability to provide both aerobic and anaerobic conditions at the same time as required for nitrification and denitrification processes.[18] In the mesocosm-scale horizontal subsurface flow constructed wetlands, the DO values were quite low in the systems, indicating more anaerobic or facultative anaerobic conditions that could suppress the growth of ammonia-oxidizing bacteria and archaea and be conducive to the development of denitrifying bacteria meanwhile.

Indeed, the sequencing of nitrogen-cycle microorganisms in the substrates of CWs showed more diverse denitrification microorganisms than the nitrification microorganisms in genus level in the substrates of CWs (Fig. 5). Furthermore, the diversity of nitrogen-cycle microorganism was related to wetland design parameters, especially the substrate type (Fig. 4). For the better understanding of microbial diversity affected by substrate type, the morphology of substrate particles was measured with field-emission scanning electron microscope (FE-SEM, ZEISS ULTRA 55, Germany) (Fig. A4) and Fourier transform infrared spectroscopy (FTIR, Bruker TENSOR 27, UK) (Fig. A5). The results showed that the ceramic had macropore structure (according to IUPAC classification for mineral pores with < 2 nm as micropores, 2–50 nm as mesopores and > 50 nm as macropores). The t macropore structures in the ceramic substrate provided the highest surface area for microbial attachment, which led to the highest OTUs. Zeolite and medical stone showed similar nitrogen-cycle microbial communities since both substrates had well-ordered lamellar structure and porous morphology. Among the four substrates investigated, only zeolite showed both microporous structures

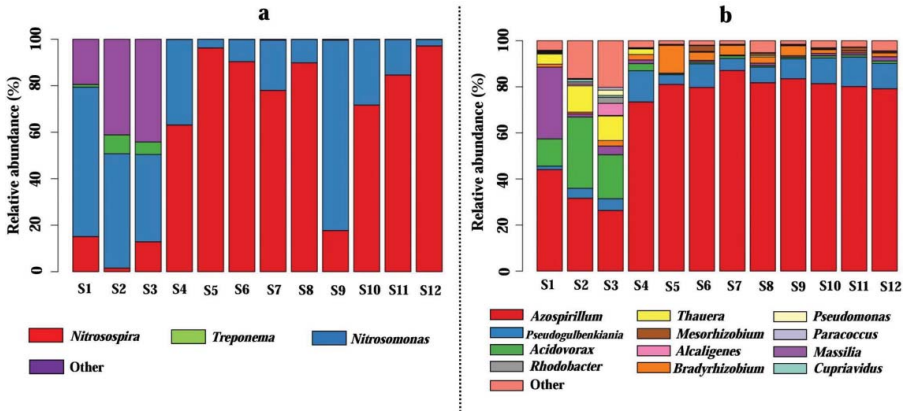

Figure 5 Microbial composition and abundance in genus level of (a) nitrification and (b) denitrification from the mesocosm-scale constructed wetlands. Sx represents substrate sample from constructed wetland CWx: CW1 (S1), CW2 (S2), CW3 (S3), CW4 (S4), CW5 (S5), CW6 (S6), CW7 (S7), CW8 (S8), CW9 (S9), CW10 (S10), CW11 (S11), CW12 (S12).

Table 3. Correlations between removal rates of nitrogenous substances (%) and gene amounts (copies/unit) of the mesocosm-scale constructed wetlands by Spearman correlation analysis.

		Removal rates of nitrogenous substances (%)			
		TN[b]	NH_3-N[c]	NO_3^-[d]	NO_2^-[e]
Gene amounts (copies/unit)	16S rRNA (bacteria)	−0.31[a]	−0.08	−0.38	0.29
	16S rRNA (archaea)	−0.21	−0.18	0.34	−0.20
	AOA	−0.09	−0.27	0.72**	−0.06
	AOB	0.25	−0.09	0.40*	−0.19
	nirS	−0.28	−0.22	−0.30	−0.44
	nirK	−0.41	−0.23	0.23	−0.31

[a]Spearman correlation coefficient (r); *Significant correlation at the 0.05 level (2-tailed); **Significant correlation at the 0.01 level (2-tailed); [b]total nitrogen; [c]ammonia nitrogen; [d]nitrate nitrogen; [e]nitrite nitrogen.

and bridging hydroxyls (Si-OH) as demonstrated by the SEM and FTIR. Microporous structures in zeolite can provide a high surface area for chemical sorption and microbial attachment, while bridging hydroxyls are catalytically active for various chemical reactions. This may explain that the highest diversity for denitrification microorganisms was found in the CWs with zeolite as substrate and the highest nitrogen removal rate was observed in the present study.

Moreover, the present study found that the abundance of denitrification genes *nirS* and *nirK* was much higher than the nitrification genes AOA and AOB (Fig. 3), indicating a more active denitrification process when compared with nitrification process. In addition, *nirS* was found more abundant than *nirK* in the CWs, suggesting that more important role for *nirS* in the denitrification process in the wastewater treatment by mesocosm-scale CWs. Nitrite reductase is the key enzyme in the dissimilatory denitrification process, and *nirS* has been reported to be more widely distributed than *nirK* in the environment.[34,48–50]

In the present study, significant positive correlations were observed between the removal rates of NO_3^- and the abundance of AOA and AOB (Table 3). Tanner and Kadlec[51] also found that the limiting step in the removal of nitrogenous substances in constructed wetlands is often not denitrification but nitrification. The present study found that *Nitrosomonas* and *Nitrosospira* genus were responsible for low-DO nitrification in the CWs (Fig. 5). These two microorganisms have been previously reported in activated sludge process.[52,53] Thus, for constructed wetlands, improving nitrification process is the key to achieve higher removal efficiency of nitrogenous substances.

Some previous studies showed that artificial aeration (continuous and intermittent mode) and combination of wetlands with different flow types called hybrid constructed wetlands, especially combination of vertical subsurface flow and horizontal subsurface flow CWs, may create alternate aerobic and anaerobic conditions in CWs to improve nitrification process.[54–56] Ong et al.[54] showed that NH_3-N removal rates in the aerated wetland reactors (98%) were better than the non-aerated wetland reactors (59–85%) because of the enhanced nitrification. Previous studies reported that hybrid constructed wetlands presented satisfactory performance of TN and NH_3-N, as the hybrid wetlands can make utilization of the nitrification ability of vertical subsurface flow CWs and the denitrification ability of horizontal subsurface flow CWs.[54,56–58] Four-month experiments showed that the wetland-applied intermittent aeration combined with step feeding strategy greatly improved the removal of ammonium nitrogen and total nitrogen simultaneously, which were 96% and 82%, respectively. It was much better than non-aerated reactors and reactors without step feeding (41–97% for NH_3-N and 29–74% for TN).[58] In addition, recirculation and step feeding can effectively improve the supply of carbon source to nitrification and denitrification of nitrogen-cycle microorganism.[59,60] Therefore, more research is needed to understand the processes associated with the combination of two or more methods (artificial aeration, combination of wetlands, recirculation and step feeding) in CWs.

Conclusion

The present study showed that the CWs with zeolite as substrate and HLR of 20 cm/d was found to be the best choice for the TN and NH_3-N removal. The microorganism community diversity and structure including nitrogen-cycle microorganisms in the constructed wetland systems were affected by the design parameters especially the substrate type. More active denitrification process was observed in these CWs as demonstrated by the more abundant denitrification genes (*nir*S and *nir*K) than the nitrification genes (AOA and AOB), and more diverse denitrification microorganisms than the nitrification microorganisms in the systems. It was found that the single-stage mesocosm-scale CWs without aeration were incapable to achieve high removals of TN and NH3-N. Nitrification is the limiting factor for the nitrogen removal by CWs. Future research is needed to improve the performance of constructed wetland systems in the nitrogen removal treatment. Research should be directed to the effects of improved technologies such as artificial aeration (continuous and intermittent mode), combination of wetlands, recirculation and step feeding.

Funding

The authors would like to acknowledge the financial support from Guangzhou municipal government (20150401007 and PC2015) and the Chinese Academy of Sciences (KZZD-EW-09). This is a Contribution No. IS-2368 from GIG CAS.

References

[1] Hu, Y.S.; Zhao, Y.Q.; Zhao, X.H.; Kumar, J.L. High rate nitrogen removal in an alum sludge-based intermittent aeration constructed wetland. Environ. Sci. Technol. **2012**, *46*, 4583–4590.

[2] Li, H.B.; Li, Y.H.; Gong, Z.Q.; Li, X.D. Performance study of vertical flow constructed wetlands for phosphorus removal with water quenched slag as a substrate. Ecol. Eng. **2013**, *53*, 39–45.

[3] Wang, Z.; Dong, J.; Liu, L.; Zhu, G.F.; Liu, C.X. Study of oyster shell as a potential substrate for constructed wetlands. Water Sci. Technol. **2013**, *67*(10), 2265–2272.

[4] Chen, J.; Liu, Y.S.; Su, H.C.; Ying, G.G.; Liu, F.; Liu, S.S.; He, L.Y.; Chen, Z.F.; Yang, Y.Q.; Chen, F.R. Removal of antibiotics and antibiotic resistance genes in rural wastewater by an integrated constructed wetland. Environ. Sci. Pollut. Res. **2014a**, *22*, 1794–1803.

[5] Chen, J.; Wei, X.D.; Liu, Y.S.; Ying, G.G.; Liu, S.S.; He, L.Y.; Su, H.C.; Hu, L.X.; Chen, F.R.; Yang, Y.Q. Removal of antibiotics and antibiotic resistance genes from domestic sewage by constructed wetlands: Optimization of wetland substrates and hydraulic loading. Sci. Total. Environ. **2016**, *565*, 240–248.

[6] Zhang, H.C.; Weber, E.J. Identifying indicators of reactivity for chemical reductants in sediments. Environ. Sci. Technol. **2012**, *47*, 6959–6968.

[7] Arroyo, P.; Ansola, G.; Sáenz de Miera, L.E. Effects of substrate, vegetation and flow on arsenic and zinc removal efficiency and microbial diversity in constructed wetlands. Ecol. Eng. **2013**, *51*, 95–103.

[8] Chen, Y.; Wen, Y.; Tang, Z.; Li, L.; Cai, Y.; Zhou, Q. Removal processes of disinfection byproducts in subsurface-flow constructed wetlands treating secondary effluent. Water Res. **2014b**, *51*, 163–171.

[9] Li, F.M.; Lu, L.; Zheng, X.; Zhang, X.W. Three-stage horizontal subsurface flow constructed wetlands for organics and nitrogen removal: effect of aeration. Ecol. Eng. **2014**, *68*, 90–96.

[10] Hijosa-Valsero, M.; Fink, G.; Schlüsener, M.P.; Sidrach-Cardona, R.; Martín-Villacorta, J.; Ternes, T.; Bécares, E. Removal of antibiotics from urban wastewater by constructed wetland optimization. Chemosphere **2011**, *83*, 713–719.

[11] Saeed, T.; Sun, G.Z. A review on nitrogen and organics removal mechanisms in subsurface flow constructed wetlands: dependency on environmental parameters, operating conditions and supporting media. J. Environ. Manage. **2012**, *112*, 429–448.

[12] Weerakoon, G.; Jinadasa, K.; Herath, G.; Mowjood, M.; Van Bruggen, J. Impact of the hydraulic loading rate on pollutants removal in tropical horizontal subsurface flow constructed wetlands. Ecol. Eng. **2013**, *61*, 154–160.

[13] Wu, S.B.; Kuschk, P.; Brix, H.; Vymazal, J.; Dong, R.J. Development of constructed wetlands in performance intensifications for wastewater treatment: a nitrogen and organic matter targeted review. Water Res. **2014**, *57*, 40–55.

[14] Wu, H.M.; Zhang, J.; Ngo, H.H.; Guo, W.S.; Hu, Z.; Liang, S.; Fan, J. L.; Liu, H. A review on the sustainability of constructed wetlands for wastewater treatment: Design and operation. Bioresour. Technol. **2015**, *175*, 594–601.

[15] Vymazal, J. Removal of nutrients in various types of constructed wetlands. Sci. Total. Environ. **2007**, *380*, 48–65.

[16] Ayaz, S. C.; Aktaş, Ö.; Fındık, N.; Akça, L.; Kınacı, C. Effect of recirculation on nitrogen removal in a hybrid constructed wetland system. Ecol. Eng. **2012**, *40*, 1–5.

[17] Cao, W.P.; Wang, Y.M.; Sun, L.; Jiang, J.L.; Zhang, Y.Q. Removal of nitrogenous compounds from polluted river water by floating constructed wetlands using rice straw and ceramsite as substrates under low temperature conditions. Ecol. Eng. **2016**, *88*, 77–81.

[18] Verhoeven, J.T.; Meuleman, A.F. Wetlands for wastewater treatment: opportunities and limitations. Ecol. Eng. **1999**, *12*, 5–12.

[19] Kadlec, R.H.; Knight, R.L.; Vymazal, J.; Brix, H.; Cooper, P.; Haberl, R. *Constructed Wetlands for Pollution Control*, International Water Association Publishing: London, UK, 2000.

[20] Kuschk, P.; Wieβner, A.; Kappelmeyer, U.; Weiβbrodt, E.; Kästner, M.; Stottmeister, U. Annual cycle of nitrogen removal by a pilot-scale subsurface horizontal flow in a constructed wetland under moderate climate. Water Res. **2003**, *37*, 4236–4242.

[21] Reinhardt, M.; Müller, B.; Gächter, R.; Wehrli, B. Nitrogen removal in a small constructed wetland: an isotope mass balance approach. Environ. Sci. Technol. **2006**, *40*(10), 3313–3319.

[22] Molle, P.; Prost-Boucle, S.; Lienard, A. Potential for total nitrogen removal by combining vertical flow and horizontal flow constructed wetlands: a full-scale experiment study. Ecol. Eng. **2008**, *34*, 23–29.

[23] Jetten, M.S.M.; Logemann, S.; Muyzer, G.; Robertson, L.A.; de Vries, S.; van Loosdrecht, M.C.; Kuenen, J.G. Novel principles in the microbial conversion of nitrogen compounds. Anton. Leeuw. Int. J. G. **1997**, *71*, 75–93.

[24] Francis, C.A.; Roberts, K.J.; Beman, J.M.; Santoro, A.E.; Oakley, B.B. Ubiquity and diversity of ammonia-oxidizing archaea in water columns and sediments of the ocean. Proc. Natl. Acad. Sci. USA. **2005**, *102*(41), 14683–14688.

[25] Ingalls, A.E.; Shah, S.R.; Hansman, R.L.; Aluwihare, L.I.; Santos, G. M.; Druffel, E.R.; Pearson, A. Quantifying archaeal community autotrophy in the mesopelagic ocean using natural radiocarbon. Proc. Natl. Acad. Sci. USA. **2006**, *103*(17), 6442–6447.

[26] Wuchter, C.; Abbas, B.; Coolen, M.J.; Herfort, L.; van Bleijswijk, J.; Timmers, P.; Strous, M.; Teira, E.; Herndl, G.J.; Middelburg, J.J.; Schouten, S.; Damsté, J.S.S. Archaeal nitrification in the ocean. Proc. Natl. Acad. Sci. USA. **2006**, *103*(33), 12317–12322.

[27] Park, H.D.; Wells, G.F.; Bae, H.; Criddle, C.S.; Francis, C.A. Occurrence of ammonia-oxidizing archaea in wastewater treatment plant bioreactors. Appl. Environ. Microb. **2006**, *72*(8), 5643–5647.

[28] You, J.; Das, A.; Dolan, E.M.; Hu, Z.Q. Ammonia-oxidizing archaea involved in nitrogen removal. Water Res. **2009**, *43*, 1801–1809.

[29] Leininger, S.; Urich, T.; Schloter, M.; Schwark, L.; Qi, J.; Nicol, G.; Prosser, J.; Schuster, S.; Schleper, C. Archaea predominate among ammonia-oxidizing prokaryotes in soils. Nature **2006**, *442*(7104), 806–809.

[30] Tourna, M.; Freitag, T.E.; Nicol, G.W.; Prosser, J.I. Growth, activity and temperature responses of ammonia-oxidizing archaea and bacteria in soil microcosms. Environ. Microbiol. **2008**, *10*(5), 1357–1364.

[31] Wang, S.Y.; Wang, Y.; Feng, X.J.; Zhai, L.M.; Zhu, G.B. Quantitative analyses of ammonia-oxidizing archaea and bacteria in the sediments of four nitrogen-rich wetlands in China. Appl. Microbiol. Biot. **2011**, *90*, 779–787.

[32] Sims, A.; Horton, J.; Gajaraj, S.; McIntosh, S.; Miles, R.J.; Mueller, R.; Reed, R.; Hu, Z. Temporal and spatial distributions of ammonia-oxidizing archaea and bacteria and their ratio as an indicator of oligotrophic conditions in natural wetlands. Water Res. **2012**, *46*, 4121–4129.

[33] Chon, K.; Chang, J.S.; Lee, E.; Lee, J.; Ryu, J.; Cho, J. Abundance of denitrifying genes coding for nitrate (narG). nitrite (nirS), and nitrous oxide (nosZ) reductases in estuarine versus wastewater effluent-fed constructed wetlands. Ecol. Eng. **2011**, *37*, 64–69.

[34] Horn, M.A.; Drake, H.L.; Schramm, A. Nitrous oxide reductase genes (nosZ) of denitrifying microbial populations in soil and the earthworm gut are phylogenetically similar. Appl. Environ. Microb. **2006**, *72*(2), 1019–1026.

[35] Standardization Administration of the People's Republic of China. Water quality-Determination of total nirtrogen-Alkline potassium persulfate digestion UV spectrophotometric method (HJ 636–2012). **2012**. Available at http://down.foodmate.net/standard/sort/9/29921.html (accessed Jan 2017).

[36] Standardization Administration of the People's Republic of China. Water quality- Determination of ammonia nitrogen-Salicylic acid spectrophotometry (HJ 536-2009). 2009. Available at http://down.foodmate.net/standard/sort/9/21845.html (accessed Jan 2017).

[37] Standardization Administration of the People's Republic of China. Water quality- Determination of nitrate-Spectrophotometric method with phenol disulfonic acid (GB/T 7480-1987). 1987. Available at http://down.foodmate.net/standard/sort/3/28916.html (accessed Jan 2017).

[38] Standardization Administration of the People's Republic of China. Water quality- Determination of nitrogen (nitrite)-Spectrophotometric method (GB/T 7480-1987). 1987. Available at http://down.foodmate.net/standard/sort/3/11644.html (accessed Jan 2017).

[39] Su, H.C.; Ying, G.G.; Tao, R.; Zhang, R.Q.; Zhao, J.L., Liu, Y.S. Class 1 and 2 integrons, sul resistance genes and antibiotic resistance in Escherichia coli isolated from Dongjiang River, South China. Environ. Pollut. **2012**, *169*, 42–49.

[40] Su, H.C.; Pan, C.G.; Ying, G.G.; Zhao, J.L.; Zhou, L.J.; Liu, Y.S.; Tao, R.; Zhang, R.Q.; He, L.Y. Contamination profiles of antibiotic resistance genes in the sediments at a catchment scale. Sci. Total. Environ. **2014**, *490*, 708–714.
[41] Beman, J.M.; Francis, C.A. Diversity of ammonia-oxidizing archaea and bacteria in the sediments of a hypernutrified subtropical estuary: Bahía del Tóbari, Mexico. Appl. Environ. Microb. **2006**, *72*(12), 7767–7777.
[42] Anceno, A.J.; Rouseau, P.; Béline, F.; Shipin, O.V.; Dabert, P. Evolution of N-converting bacteria during the start-up of anaerobic digestion coupled biological nitrogen removal pilot-scale bioreactors treating high-strength animal waste slurry. Bioresour. Tchenol. **2009**, *100*(14), 3678–3687.
[43] Chao, A. Nonparametric estimation of the number of classes in a population. Scand. J. Stat. **1984**, *11*, 265–270.
[44] Chao, A.; Shen, T.J. Nonparametric estimation of Shannon's index of diversity when there are unseen species in sample. Environ. Ecol. Stat. **2003**, *10*, 429–443.
[45] Faith, D.P. Systematics and conservation: on predicting the feature diversity of subsets of taxa. Cladistics **1992**, *8*, 361–373.
[46] Fierer, N.; Jackson, R.B. The diversity and biogeography of soil bacterial communities. Proc. Natl. Acad. Sci. USA. **2006**, *103*(3), 626–631.
[47] Forest, F.; Grenyer, R.; Rouget, M.; Davies, T.J.; Cowling, R.M.; Faith, D.P.; Balmford, A.; Manning, J.C.; Procheş, Ş.; van der Bank, M. Preserving the evolutionary potential of floras in biodiversity hotspots. Nature **2007**, *445*(7129), 757–760.
[48] Braker, G.; Fesefeldt, A.; Witzel, K.P. Development of PCR primer systems for amplification of nitrite reductase genes (nirK and nirS) to detect denitrifying bacteria in environmental samples. Appl. Environ. Microb. **1998**, *64*(10), 3769–3775.
[49] Kandeler, E.; Deiglmayr, K.; Tscherko, D.; Bru, D.; Philippot, L. Abundance of narG, nirS, nirK, and nosZ genes of denitrifying bacteria during primary successions of a glacier foreland. Appl. Environ. Microb. **2006**, *72*(9), 5957–5962.
[50] Park, H.D.; Noguera, D.R. Evaluating the effect of dissolved oxygen on ammonia-oxidizing bacterial communities in activated sludge. Water Res. **2004**, *38*, 3275–3286.
[51] Fitzgerald, C.M.; Camejo, P.; Oshlag, J.Z.; Noguera, D.R. Ammonia-oxidizing microbial communities in reactors with efficient nitrification at low-dissolved oxygen. Water Res. **2015**, *70*, 38–51.
[52] Tanner, C.; Kadlec, R. Oxygen flux implications of observed nitrogen removal rates in subsurface-flow treatment wetlands. Water Sci. Technol. **2003**, *48*(5), 191–198.
[53] Gaboutloeloe, G. K.; Chen, S.; Barber, M. E.; Stöckle, C. O. Combinations of horizontal and vertical flow constructed wetlands to improve nitrogen removal. Water Air Soil Pollut. **2009**, *9*, 279–286.
[54] Ong, S. A.; Uchiyama, K.; Inadama, D.; Ishida, Y.; Yamagiwa, K. Performance evaluation of laboratory scale up-flow constructed wetlands with different designs and emergent plants. Bioresour. Technol. **2010**, *101*, 7239–7244.
[55] Vymazal, J. The use of hybrid constructed wetlands for wastewater treatment with special attention to nitrogen removal: a review of a recent development. Water Res. **2013**, *47*, 4795–4811.
[56] Cooper, P. A review of the design and performance of vertical-flow and hybrid reed bed treatment systems. Water Sci. Technol. **1999**, *40*(3), 1–9.
[57] Abidi, S.; Kallali, H.; Jedidi, N.; Bouzaiane, O.; Hassen, A. Comparative pilot study of the performances of two constructed wetland wastewater treatment hybrid systems. Desalination **2009**, *246*, 370–377.
[58] Fan, J.L.; Liang, S.; Zhang, B.; Zhang, J. Enhanced organics and nitrogen removal in batch-operated vertical flow constructed wetlands by combination of intermittent aeration and step feeding strategy. Environ. Sci. Pollut. Res. **2013**, *20*, 2448–2455.
[59] Duan, Q.J.; Shang, S.Q.; Wu, Y.D. Rapid diagnosis of bacterial meningitis in children with fluorescence quantitative polymerase chain reaction amplification in the bacterial 16S rRNA gene. Eur. J. Pediatr. **2009**, *168* (2), 211–216.
[60] Sun, D. L.; Jiang, X.; Wu, Q. L.; Zhou, N. Y. Intragenomic heterogeneity of 16S rRNA genes causes overestimation of prokaryotic diversity. Appl. Environ. Microbiol. **2013**, *79*(19), 5962–5969.

Appendix

Text A1 Nitrogen-cycle genes quantification

Real-time quantitative polymerase chain reaction (qPCR) was used to quantify the six target genes including the 16S ribosomal RNA (16S rRNA) of bacteria and archaea, and four nitrogen-cycle genes, that is ammonia monooxygenase (amoA) of bacteria (AOB) and archaea (AOA) and nitrite reductase (nirK and nirS). The ViiA 7 Real-Time PCR System (ABI, USA) using SYBR Green Real-Time QPCR Kit (TAKARA, Japan) was applied to quantitatively determine the abundance of resistance genes. Both positive and negative controls (Milli-Q water) were included in every run. Positive controls consisted of cloned and sequenced PCR amplicons obtained from the sludge of WWTPs and manure of livestock farms. A total of 40 cycles was applied to improve the chances of product formation from low initial template concentrations. A 20-μL PCR reaction solution was employed: 2× THUNDERBIRD SYBR® qPCR Mix 10 μL, 0.05 mM each primer 0.08 μL, 50× ROX reference dye 0.04 μL, template DNA 2 μL (DNA $<$ 80 ng), and distilled water 7.8 μL (DNase I treated). The qPCR assays were run on an Applied Biosystems 7500 Fast Real-Time PCR System (ABI, USA). The temperature program for quantification of ARGs consisted of initial denaturing at 95°C for 1 min, followed by 40 cycles for 15 s at 95°C, 55°C for 30 s (some primers of ARGs have different annealing temperatures, see Table S1), 72°C for 30 s, and a final step for melting curve. The external reference method was used to calculate the copy number of ARGs, with the square of related coefficient (r2) of the standard curve $>$0.99 and the amplification efficiency ranging between 95% and 110%.

Table A1. Primers used in this study for quantitative PCR.

Gene	Primer pair [a]	Sequences (5′→3′)	Annealing temp (°C)	Amplicon size (bp)	Reference
16S rRNA (bacteria)	FW	TGTGTAGCGGTGAAATGCG	62	140	[1]
	RV	CATCGTTTACGGCGTGGAC			
16S rRNA (archaea)	FW	ACKGCCAGTAACACGT	57	225	[2]
	RV	TCGCGCCTGCTGCTCCCCGT			
AOA	FW	STAATGGTCTGGCTTAGACG	53	635	[3]
	RV	GCGGCCATCCATCTGTATGT			
AOB	FW	GGGGTTTCTACTGGTGGT	55	491	[4]
	RV	CCCCTCKGSAAAGCCTTCTTC			
nirK	FW	GGMATGGTKCCSTGGCA	58	514	[5]
	RV	GCCTCGATCAGRTTRTGGTT			
nirS	FW	GTSAACGTSAAGGARACSGG	57	425	[5]
	RV	GASTTCGGRTGSGTCTTGA			

[a]FW, forward; RV, reverse.

Table A2. Wastewater quality parameters in influent and effluents of the mesocosm-scale constructed wetlands.

			Temperature (°C)	PH	DO[a] (mg/L)	Conductivity (μs/cm)	Redox potential (mV)
Influent			17.9 ± 0.60	7.96 ± 0.03	0.22 ± 0.07	130 ± 11.1	155 ± 5.04
Effluents	Oyster shell	HLR = 10 [b]	14.8 ± 1.01	8.06 ± 0.04	0.72 ± 0.15	115 ± 7.55	162 ± 8.97
		HLR = 20	15.0 ± 1.16	8.03 ± 0.03	0.47 ± 0.07	114 ± 6.75	153 ± 9.25
		HLR = 30	15.1 ± 1.06	8.01 ± 0.02	0.57 ± 0.06	113 ± 5.99	151 ± 7.18
	Zeolite	HLR = 10	14.9 ± 0.96	8.06 ± 0.06	0.65 ± 0.13	111 ± 7.37	157 ± 11.9
		HLR = 20	15.0 ± 1.08	8.02 ± 0.04	0.65 ± 0.07	111 ± 6.98	154 ± 11.0
		HLR = 30	15.5 ± 1.10	8.04 ± 0.02	0.64 ± 0.08	114 ± 8.41	156 ± 22.9
	Medical stone	HLR = 10	15.2 ± 1.27	8.13 ± 0.05	0.50 ± 0.08	117 ± 10.1	165 ± 11.8
		HLR = 20	15.1 ± 1.22	8.03 ± 0.03	0.47 ± 0.10	117 ± 8.93	154 ± 5.64
		HLR = 30	15.5 ± 1.37	7.93 ± 0.03	0.70 ± 0.10	119 ± 8.69	150 ± 4.00
	Ceramic	HLR = 10	15.2 ± 1.26	8.16 ± 0.03	0.48 ± 0.07	121 ± 9.22	178 ± 4.52
		HLR = 20	15.3 ± 1.21	8.07 ± 0.03	0.44 ± 0.07	121 ± 8.56	162 ± 5.37
		HLR = 30	15.4 ± 1.28	8.03 ± 0.02	0.65 ± 0.09	123 ± 8.18	160 ± 4.96

[a]Dissolved oxygen; [b]hydraulic loading rate (cm/d).

Table A3. Absolute concentrations (copies/mL) of nitrogen-cycle genes in the influent and effluents of mesocosm-scale constructed wetlands.

			16S rRNA (bacteria)	16S rRNA (archaea)	AOA	AOB	*nirS*	*nirK*
Influent			$(8.73 \pm 1.71) \times 10^{9}$[a]	$(8.87 \pm 3.05) \times 10^{7}$	$(2.92 \pm 0.65) \times 10^{5}$	$(3.58 \pm 0.84) \times 10^{5}$	$(1.86 \pm 0.98) \times 10^{9}$	$(1.08 \pm 0.36) \times 10^{6}$
Effluents	Oyster shell	HLR = 10[b]	$(4.39 \pm 1.36) \times 10^{9}$	$(1.52 \pm 0.22) \times 10^{7}$	$(2.43 \pm 0.34) \times 10^{5}$	$(1.19 \pm 0.65) \times 10^{5}$	$(1.60 \pm 0.19) \times 10^{8}$	$(2.28 \pm 1.44) \times 10^{5}$
		HLR = 20	$(7.29 \pm 5.27) \times 10^{9}$	$(2.86 \pm 1.32) \times 10^{7}$	$(3.34 \pm 0.75) \times 10^{5}$	$(7.25 \pm 0.71) \times 10^{5}$	$(6.99 \pm 0.71) \times 10^{8}$	$(5.21 \pm 0.39) \times 10^{5}$
		HLR = 30	$(8.10 \pm 0.71) \times 10^{9}$	$(3.88 \pm 1.00) \times 10^{7}$	$(3.33 \pm 0.62) \times 10^{5}$	$(1.84 \pm 0.99) \times 10^{5}$	$(3.19 \pm 0.58) \times 10^{8}$	$(3.31 \pm 0.96) \times 10^{5}$
	Zeolite	HLR = 10	$(1.81 \pm 0.75) \times 10^{9}$	$(1.52 \pm 1.19) \times 10^{7}$	$(2.62 \pm 0.46) \times 10^{5}$	$(1.29 \pm 0.98) \times 10^{5}$	$(1.21 \pm 0.85) \times 10^{8}$	$(1.54 \pm 1.04) \times 10^{5}$
		HLR = 20	$(4.48 \pm 2.61) \times 10^{9}$	$(7.86 \pm 5.48) \times 10^{6}$	$(3.23 \pm 0.40) \times 10^{5}$	$(2.01 \pm 0.23) \times 10^{5}$	$(7.17 \pm 0.64) \times 10^{8}$	$(5.15 \pm 0.52) \times 10^{5}$
		HLR = 30	$(3.85 \pm 1.92) \times 10^{9}$	$(8.84 \pm 5.30) \times 10^{6}$	$(1.85 \pm 0.25) \times 10^{5}$	$(1.44 \pm 0.52) \times 10^{5}$	$(6.69 \pm 1.09) \times 10^{8}$	$(4.38 \pm 0.16) \times 10^{5}$
	Medical stone	HLR = 10	$(4.22 \pm 1.56) \times 10^{9}$	$(5.57 \pm 4.08) \times 10^{7}$	$(2.55 \pm 0.49) \times 10^{5}$	$(8.48 \pm 6.68) \times 10^{5}$	$(8.62 \pm 0.63) \times 10^{8}$	$(6.98 \pm 0.48) \times 10^{5}$
		HLR = 20	$(5.20 \pm 3.13) \times 10^{9}$	$(4.06 \pm 2.83) \times 10^{7}$	$(3.34 \pm 1.07) \times 10^{5}$	$(5.04 \pm 4.62) \times 10^{5}$	$(2.39 \pm 0.16) \times 10^{9}$	$(2.59 \pm 0.16) \times 10^{6}$
		HLR = 30	$(5.94 \pm 0.11) \times 10^{9}$	$(3.22 \pm 1.16) \times 10^{7}$	$(2.85 \pm 2.17) \times 10^{5}$	$(2.70 \pm 1.45) \times 10^{5}$	$(1.13 \pm 0.66) \times 10^{9}$	$(6.67 \pm 0.16) \times 10^{5}$
	Ceramic	HLR = 10	$(4.36 \pm 0.93) \times 10^{9}$	$(5.13 \pm 1.64) \times 10^{7}$	$(2.95 \pm 0.38) \times 10^{5}$	$(7.07 \pm 1.49) \times 10^{5}$	$(1.55 \pm 8.30) \times 10^{9}$	$(9.69 \pm 0.63) \times 10^{5}$
		HLR = 20	$(3.52 \pm 1.48) \times 10^{9}$	$(2.31 \pm 1.37) \times 10^{7}$	$(3.46 \pm 0.88) \times 10^{5}$	$(1.99 \pm 0.91) \times 10^{5}$	$(7.37 \pm 5.23) \times 10^{8}$	$(6.61 \pm 0.23) \times 10^{5}$
		HLR = 30	$(4.40 \pm 0.83) \times 10^{9}$	$(2.78 \pm 0.41) \times 10^{7}$	$(2.17 \pm 1.38) \times 10^{5}$	$(1.53 \pm 1.26) \times 10^{5}$	$(8.95 \pm 1.15) \times 10^{8}$	$(2.51 \pm 0.61) \times 10^{5}$

[a]mean ± standard derivation.
[b]hydraulic loading rate (cm/d).

Table A4. Absolute concentrations (copies/g) of nitrogen-cycle genes in the substrates of mesocosm-scale constructed wetlands.

		16S rRNA (bacteria)	16S rRNA (archaea)	AOA	AOB	*nirS*	*nirK*
Oyster shell	HLR = 10 [b]	$(2.66 \pm 0.14) \times 10^{7}$ [a]	$(2.60 \pm 1.01) \times 10^{7}$	$(1.99 \pm 0.55) \times 10^{5}$	$(6.64 \pm 0.02) \times 10^{5}$	$(8.26 \pm 0.36) \times 10^{7}$	$(7.97 \pm 0.39) \times 10^{5}$
	HLR = 20	$(3.12 \pm 0.50) \times 10^{7}$	$(5.77 \pm 0.01) \times 10^{6}$	$(2.33 \pm 0.14) \times 10^{5}$	$(2.99 \pm 0.15) \times 10^{5}$	$(8.58 \pm 0.01) \times 10^{7}$	$(8.11 \pm 0.01) \times 10^{5}$
	HLR = 30	$(7.16 \pm 0.02) \times 10^{7}$	$(2.45 \pm 0.08) \times 10^{7}$	$(7.69 \pm 0.25) \times 10^{5}$	$(3.88 \pm 0.69) \times 10^{5}$	$(5.43 \pm 0.46) \times 10^{7}$	$(6.36 \pm 0.39) \times 10^{5}$
Zeolite	HLR = 10	$(8.10 \pm 0.35) \times 10^{6}$	$(2.43 \pm 0.07) \times 10^{7}$	$(3.66 \pm 0.02) \times 10^{5}$	$(2.74 \pm 0.50) \times 10^{6}$	$(7.45 \pm 1.10) \times 10^{7}$	$(4.50 \pm 0.61) \times 10^{6}$
	HLR = 20	$(1.35 \pm 0.09) \times 10^{7}$	$(2.20 \pm 0.01) \times 10^{7}$	$(2.90 \pm 1.00) \times 10^{5}$	$(3.33 \pm 0.03) \times 10^{6}$	$(2.69 \pm 0.16) \times 10^{7}$	$(1.92 \pm 0.41) \times 10^{6}$
	HLR = 30	$(1.65 \pm 0.04) \times 10^{7}$	$(3.00 \pm 0.03) \times 10^{7}$	$(4.15 \pm 0.29) \times 10^{5}$	$(2.88 \pm 1.17) \times 10^{6}$	$(1.18 \pm 0.25) \times 10^{8}$	$(9.52 \pm 0.34) \times 10^{6}$
Medical stone	HLR = 10	$(6.25 \pm 0.44) \times 10^{6}$	$(3.76 \pm 0.38) \times 10^{7}$	$(2.69 \pm 1.78) \times 10^{5}$	$(8.40 \pm 0.44) \times 10^{6}$	$(9.74 \pm 2.35) \times 10^{7}$	$(4.53 \pm 0.33) \times 10^{6}$
	HLR = 20	$(1.91 \pm 0.01) \times 10^{7}$	$(4.14 \pm 0.58) \times 10^{7}$	$(3.33 \pm 0.11) \times 10^{5}$	$(2.15 \pm 0.12) \times 10^{6}$	$(4.35 \pm 1.70) \times 10^{7}$	$(8.11 \pm 0.53) \times 10^{6}$
	HLR = 30	$(5.58 \pm 0.33) \times 10^{6}$	$(2.20 \pm 0.31) \times 10^{7}$	$(3.19 \pm 0.55) \times 10^{5}$	$(2.32 \pm 0.01) \times 10^{6}$	$(2.36 \pm 0.78) \times 10^{7}$	$(1.80 \pm 0.07) \times 10^{6}$
Ceramic	HLR = 10	$(3.13 \pm 0.13) \times 10^{6}$	$(1.47 \pm 0.13) \times 10^{7}$	$(2.23 \pm 0.94) \times 10^{5}$	$(4.56 \pm 0.45) \times 10^{6}$	$(2.54 \pm 0.23) \times 10^{7}$	$(1.79 \pm 0.11) \times 10^{6}$
	HLR = 20	$(1.49 \pm 0.09) \times 10^{7}$	$(4.61 \pm 0.66) \times 10^{7}$	$(3.29 \pm 0.26) \times 10^{6}$	$(9.21 \pm 0.25) \times 10^{6}$	$(4.31 \pm 0.26) \times 10^{7}$	$(4.54 \pm 0.03) \times 10^{6}$
	HLR = 30	$(8.78 \pm 0.62) \times 10^{6}$	$(2.45 \pm 0.06) \times 10^{7}$	$(3.66 \pm 0.95) \times 10^{5}$	$(2.87 \pm 0.13) \times 10^{6}$	$(5.22 \pm 0.58) \times 10^{7}$	$(8.66 \pm 0.62) \times 10^{6}$

[a]mean ± standard derivation; [b]hydraulic loading rate (cm/d).

Table A5. Gene amounts (copies/unit) of the mesocosm-scale constructed wetlands.

		16S rRNA (bacteria)	16S rRNA (archaea)	AOA	AOB	*nirS*	*nirK*
Oyster shell	HLR = 10 [a]	8.33×10^{14}	4.83×10^{12}	6.09×10^{10}	7.23×10^{10}	3.66×10^{13}	1.03×10^{11}
	HLR = 20	1.38×10^{15}	5.86×10^{12}	8.08×10^{10}	1.60×10^{11}	1.39×10^{14}	1.60×10^{11}
	HLR = 30	1.54×10^{15}	9.20×10^{12}	1.21×10^{11}	6.40×10^{10}	6.46×10^{13}	1.10×10^{11}
Zeolite	HLR = 10	2.92×10^{14}	1.58×10^{13}	2.43×10^{11}	1.52×10^{12}	6.02×10^{13}	2.50×10^{12}
	HLR = 20	7.21×10^{14}	1.33×10^{13}	2.11×10^{11}	1.86×10^{12}	1.29×10^{14}	1.14×10^{12}
	HLR = 30	6.23×10^{14}	1.79×10^{13}	2.58×10^{11}	1.61×10^{12}	1.72×10^{14}	5.31×10^{12}
Medical stone	HLR = 10	6.53×10^{14}	2.36×10^{13}	1.47×10^{11}	3.49×10^{12}	1.72×10^{14}	1.92×10^{12}
	HLR = 20	8.09×10^{14}	2.28×10^{13}	1.85×10^{11}	9.36×10^{11}	3.85×10^{14}	3.64×10^{12}
	HLR = 30	9.18×10^{14}	1.38×10^{13}	1.72×10^{11}	9.69×10^{11}	1.84×10^{14}	8.21×10^{11}
Ceramic	HLR = 10	7.22×10^{14}	1.29×10^{13}	1.16×10^{11}	1.48×10^{12}	2.64×10^{14}	6.98×10^{11}
	HLR = 20	5.87×10^{14}	1.76×10^{13}	1.05×10^{12}	2.79×10^{12}	1.35×10^{14}	1.47×10^{12}
	HLR = 30	7.29×10^{14}	1.20×10^{13}	1.46×10^{11}	8.86×10^{11}	1.64×10^{14}	2.64×10^{12}

[a]Hydraulic loading rate (cm/d).

Table A6. The raw tags, clean tags and OTUs of the substrate samples from the mesocosm-scale CWs.

		amoA for nitrification			*nosZ* for denitrification		
		Raw tag	Clean tag	OTUs	Raw tag	Clean tag	OTUs
Oyster shell	HLR = 10[a]	21660	20591	843	50879	49828	2340
	HLR = 20	13326	13135	665	28393	26628	2761
	HLR = 30	51648	50607	1765	32527	31509	2546
Zeolite	HLR = 10	38972	33597	1394	123775	121312	5162
	HLR = 20	45979	34151	2665	109428	92169	4692
	HLR = 30	42047	34902	1871	135260	132798	4701
Medical stone	HLR = 10	93016	86171	1288	135166	131115	4800
	HLR = 20	73741	66361	3334	169236	167244	4568
	HLR = 30	140716	136280	2359	165583	163414	4261
Ceramic	HLR = 10	141656	125151	4901	125403	121700	5593
	HLR = 20	70537	62669	3628	162406	157483	5840
	HLR = 30	170984	151458	5926	174128	172171	5775

[a]Hydraulic loading rate (cm/d).

Table A7. Alpha diversity analysis results of the substrate samples from the mesocosm-scale CWs.

		amoA for nitrification				*nosZ* for denitrification			
		Chao1	Observed species	PD, whole tree	Shannon	Chao1	Observed species	PD, whole tree	Shannon
Oyster shell	HLR = 10[a]	1092	725	167	6.29	2744	1650	200	5.75
	HLR = 20	679	665	312	7.03	4780	2756	144	8.27
	HLR = 30	1688	1072	278	7.87	4692	2705	154	8.14
Zeolite	HLR = 10	1553	946	11.7	7.14	4629	2657	175	8.59
	HLR = 20	2864	1951	4.99	9.21	3757	2758	345	8.76
	HLR = 30	2165	1263	9.70	8.11	3254	2363	378	8.67
Medical stone	HLR = 10	1140	573	29.1	6.33	4344	2575	122	8.42
	HLR = 20	3025	1778	11.5	9.46	4450	2733	99.3	8.59
	HLR = 30	1508	820	36.4	5.69	3892	2170	93.9	7.60
Ceramic	HLR = 10	3501	2134	24.2	9.11	4366	2301	90.9	7.81
	HLR = 20	3247	2005	16.7	9.36	3645	2008	94.8	7.91
	HLR = 30	4237	2647	31.4	9.90	3392	1858	102	7.57

[a]Hydraulic loading rate (cm/d).

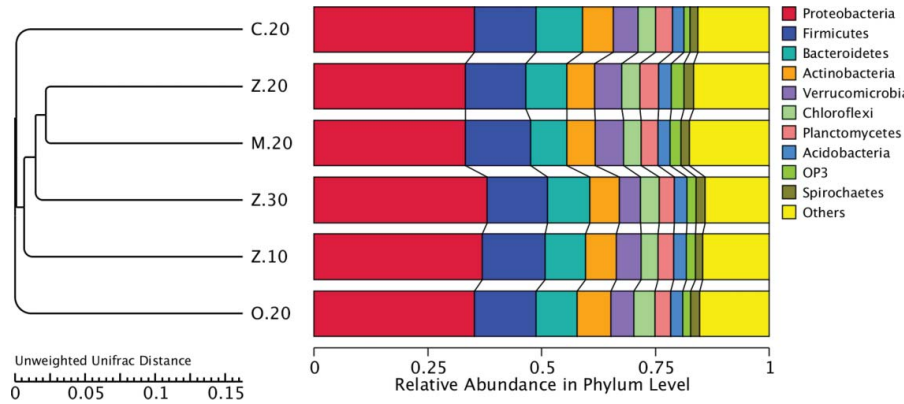

Figure A1. UPGMA (unweighted pair-group method with Arithmetic Mean) analysis based on the Weighted UniFrac distance in phylum level from the mesocosm-scale constructed wetlands. CW-O-20 (S2), CW-Z-10 (S4), CW-Z-20 (S5), CW-Z-30 (S6), CW-M-20 (S8), CW-C-20 (S11). Sx represent substrate samples from the constructed wetland CWx.

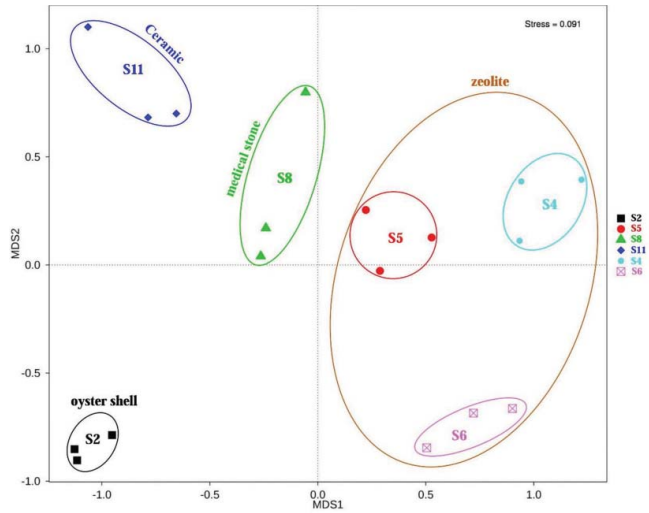

Figure A2. Non-metric multi-dimensional scaling (NMDS) analysis based on the OTUs abundances of microorganism from the mesocosm-scale constructed wetlands. CW-O-20 (S2), CW-Z-10 (S4), CW-Z-20 (S5), CW-Z-30 (S6), CW-M-20 (S8), CW-C-20 (S11).

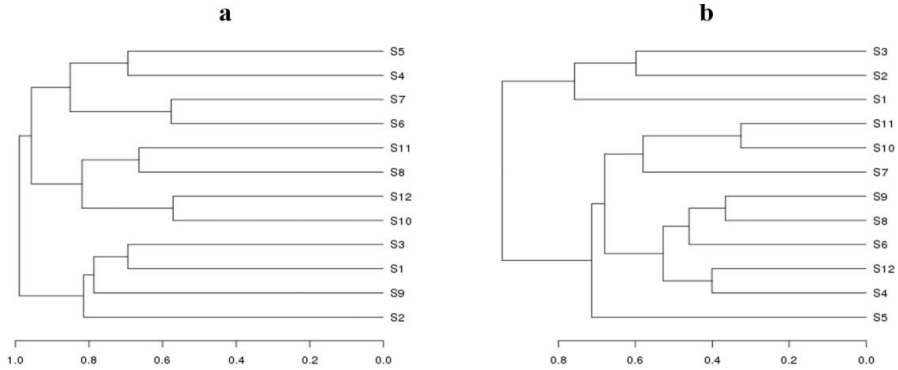

Figure A3. The cluster analysis based on the OTUs abundances of (a) nitrification and (b) denitrification from the mesocosm-scale constructed wetlands. CW-O-10 (S1), CW-O-20 (S2), CW-O-30 (S3), CW-Z-10 (S4), CW-Z-20 (S5), CW-Z-30 (S6), CW-M-10 (S7), CW-M-20 (S8), CW-M-30 (S9), CW-C-10 (S10), CW-C-20 (S11), CW-C-30 (S12).

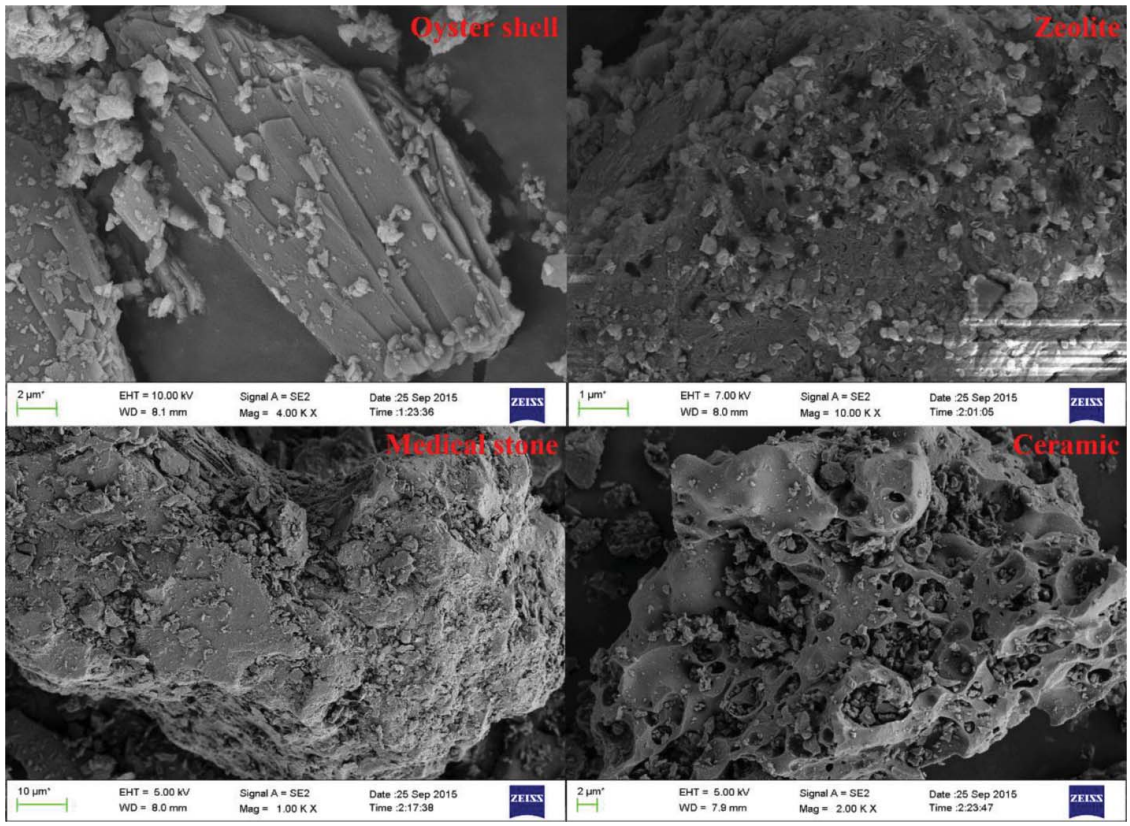

Figure A4. Pictures of the field emission scanning electron microscope for the four substrates used in the constructed wetlands.

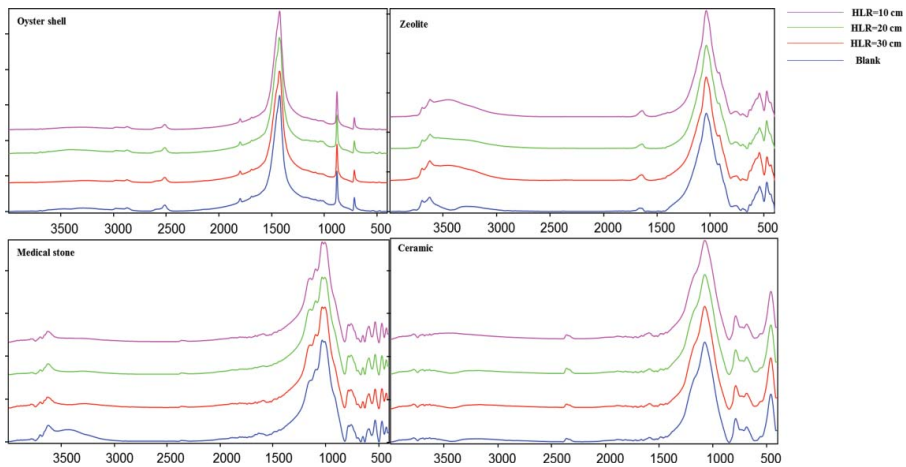

Figure A5. FTIR results of different substrates in different conditions in the mesocosm-scale constructed wetlands.